

Rapid Adjustments of Cloud and Hydrological Cycle to Increasing CO₂: a Review

Youichi Kamae · Masahiro Watanabe · Tomoo Ogura ·
Masakazu Yoshimori · Hideo Shiogama

Published online: 7 March 2015

© The Author(s) 2015. This article is published with open access at Springerlink.com

Abstract Rapid cloud response to instantaneous radiative perturbation in the troposphere due to change in CO₂ concentration is called cloud adjustment. Cloud adjustment develops on a short timescale because it is separated from surface temperature-mediated changes in cloud. Adjustments in cloud and tropospheric properties including the hydrological cycle have attracted considerable attention because of their importance in the interpretation of mechanisms of climate change and the identification of sources of uncertainty in climate sensitivity. Modeling studies have clearly revealed that major aspects of the tropospheric adjustment including the warming and drying of the troposphere, associated reduction of low cloud and increasing shortwave cloud radiative forcing, downward shift of the low-cloud layer, and slowdown of the global hydrological cycle, are common among many climate model simulations. Combinations of model simulations with realistic and idealized aqua-planet settings have helped demonstrate the roles of land and robust aspects of the tropospheric adjustment.

Keywords Climate sensitivity · Effective radiative forcing · Instantaneous radiative forcing · Land–sea thermal contrast · Low cloud · Hydrological cycle

This article is part of the Topical Collection on *Climate Feedbacks*

Y. Kamae (✉) · T. Ogura · H. Shiogama
Center for Global Environmental Research, National Institute for
Environmental Studies, 16-2 Onogawa, Tsukuba, Ibaraki 305-8506,
Japan
e-mail: kamae.yoichi@nies.go.jp

M. Watanabe
Atmosphere and Ocean Research Institute, University of Tokyo,
5-1-5 Kashiwanoha, Kashiwa, Chiba 277-8568, Japan

M. Yoshimori
Faculty of Environmental Earth Science, Hokkaido University,
N10W5, Sapporo, Hokkaido 060-0810, Japan

Introduction

Equilibrium climate sensitivity (ECS), defined as global-mean surface air temperature (SAT) change due to a doubling of atmospheric CO₂ concentration, is a metric commonly used to explore the Earth's climate response to externally induced forcing [1]. Despite the considerable efforts expended in quantifying and constraining ECS, its range of uncertainty has not been reduced effectively during these three decades [1–3]. The response of cloud properties to climate warming is one of the largest contributors to ECS uncertainty [3]. Increasing CO₂ results in a radiative perturbation that affects cloud properties directly [3–6]. This direct cloud response to increasing levels of CO₂ is independent of the global-mean SAT increase and it should be distinguished from SAT-mediated cloud changes. It has been derived from atmosphere–ocean coupled general circulation models (AOGCMs) that this cloud response, called “cloud adjustment,” generates radiative forcing of about 0.5 W m⁻² per the doubling of CO₂ concentration [7••]. This radiative effect is of great importance to the effective radiative forcing (ERF), determined by a radiative imbalance at the top of the atmosphere (TOA) without any changes in global-mean SAT under the conditions of doubled CO₂ [1, 8], and it has a non-negligible contribution to the ECS [7••, 9•, 10•].

The rapid adjustments of cloud and tropospheric properties can be interpreted as part of the direct climate response to increasing CO₂. Here, the “direct response” means the response to radiative forcing without any perturbations in sea surface temperature (SST) and sea ice. The roles of the direct climate response to radiative forcing for some aspects of climate change have been examined thoroughly (e.g., land–sea temperature contrast, atmospheric circulation [11–15, 16•, 17, 18, 19•, 20••, 21–23], and tropical cyclone activity [24–26]). Quantifying the radiative effect of the tropospheric cloud adjustment is essential for better understanding of the

uncertainty in the ECS [7•, 27–29]. It has also been widely accepted that the role of the direct response to CO₂ increase is substantial for the global hydrological cycle [19•, 20•, 21, 30–40], including evapotranspiration over land [5, 41, 42•].

The mechanism of tropospheric adjustment to increasing CO₂ has been examined using two methodologies: the fixed-SST method (Hansen method) and the regression method (Gregory method). In the fixed-SST method, ERF can be evaluated by the difference between two equilibrium states simulated in atmospheric general circulation models (AGCMs) with fixed SST and sea ice, but with differing CO₂ concentrations in the atmosphere [8, 43]. It should be noted that influences attributed to land surface warming in response to the CO₂ increase are also included within this estimate (discussed below) [44]. The timescales of the cloud adjustment to abrupt increases in CO₂ are thought to be of the order of days to weeks [1, 41]. To examine the rapid adjustment processes in the cloud and hydrological cycle, a short ensemble simulation based on the fixed-SST method has been employed [19•, 20•]. In this method, short-term and large-member ensemble simulations were performed with the AGCM 1× and 4× the concentration of atmospheric CO₂. The ensemble-means of the two model outputs are compared at a fixed lead-time (e.g., 1 day, 5 days, and so on) and their difference can be evaluated as the rapid adjustment. In the regression method, on the contrary, SST and sea ice are allowed to vary. In abrupt CO₂ concentration increase experiments of AOGCM, the decrease in TOA net radiation is approximately linear with SAT increase. The regression line is extrapolated to estimate the ERF at zero global-mean SAT change (i.e., without feedbacks) [4, 5, 29, 45]. To improve the signal-to-noise ratio, a large ensemble (>10) of integrations with abrupt increase in CO₂ is preferred to diagnose the ERF using the regression method [7•, 20•, 46]. Note that change in local SAT is not necessarily equal to zero even when the global-mean change in SAT is zero. The direct response to increasing CO₂ estimated in the regression method is influenced by the local SAT change partly [4].

Improvements in the evaluation of the rapid adjustment have provided new insights into the adjustment processes and sources of uncertainty. In this paper, the progress made by studies on the rapid adjustment and the direct climate responses to increasing CO₂ is reviewed. Note that carbon cycle feedback is not quantified in the ECS concept [1] and is not included in this paper. We focused mainly on the following: (1) the physical mechanism of adjustments in cloud and hydrological cycle, (2) timescales of the processes related to rapid adjustment, (3) role of land surface to the direct responses in the cloud and troposphere, (4) sources of uncertainty in the cloud adjustment, and (5) some applications of the concept of the direct climate response to externally induced radiative forcing. Here, the attention is on climate responses to spatially uniform CO₂ concentration increase; the influences

of horizontally inhomogeneous radiative forcing agents (e.g., aerosols) on clouds have been detailed in other papers [3, 6].

Physical Mechanisms of Adjustments in Cloud and Hydrological Cycle

Although some previous studies have estimated the longwave and shortwave components of the radiative effect of rapid cloud adjustment, the signs of the estimated forcings varied among the different studies and models (particularly in the shortwave component) [4, 29]. However, interpretations of the physical processes of the rapid cloud adjustment and the robustness of its radiative effect have improved considerably because of the increased signal-to-noise ratio associated with quantifying methodologies (see previous subsection).

Figure 1 shows the mechanism of cloud adjustment over the ocean [7•, 20•, 28]. The processes of direct responses over the land and their roles in the global-mean response are detailed later. The cloud adjustment is characterized principally by two aspects: general tropospheric drying and the downward shift of the low-cloud layer (Fig. 1). With increasing atmospheric CO₂ concentration, longwave heating of the atmosphere due to instantaneous radiative forcing [47, 48] induces general tropospheric warming, resulting in reductions of tropospheric relative humidity (RH) and cloud amount (Fig. 1) [7•, 20•, 28]. The radiative-heating-induced drying of the lower and mid-troposphere, which has been widely confirmed

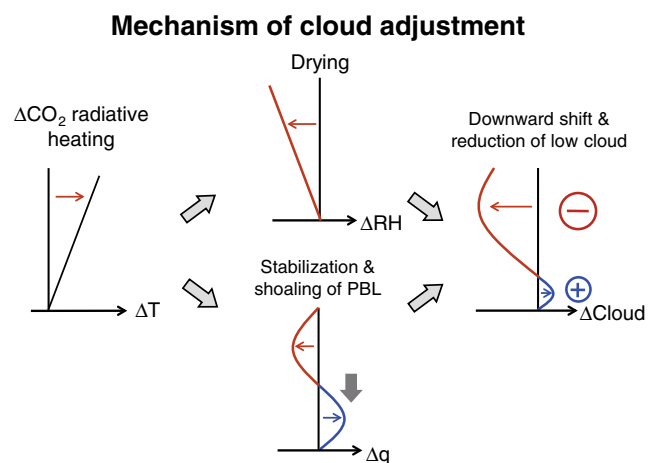


Fig. 1 Schematics of rapid adjustment of low cloud over ocean to increasing CO₂. ΔT change in atmospheric temperature, ΔRH change in relative humidity, Δq change in specific humidity, $\Delta Cloud$ change in cloud amount in the lower troposphere. Colored arrows represent changes in vertical profiles of the thermodynamic properties (ΔT , ΔRH , Δq , and $\Delta Cloud$). $\Delta Cloud$ (downward shift and reduction of low cloud) can be explained largely by sum of the effects of lower-tropospheric drying (negative ΔRH) and shoaling of marine boundary layer (negative and positive Δq in the upper and lower parts, respectively). Modified from: Kamae Y, Watanabe M (2013) Tropospheric adjustment to increasing CO₂: its timescale and the role of land–sea contrast. *Clim Dyn* 41:3007–3024

by many GCMs despite some perturbations in surface evaporation and the vertical profile of specific humidity [9•, 28, 49], results in a robust reduction of low cloud (Fig. 1) [7••, 20••, 28]. In addition to the general drying of the troposphere, vertical shifts of humidity and cloud layers are also essential parts of the cloud adjustment (Fig. 1) [7••, 20••]. In response to CO₂ increase, the following two processes occur within the lower troposphere: (1) the suppression of turbulent (sensible and latent) heat fluxes from the sea surface [35, 50] and (2) increase in static stability of the lower troposphere [20••, 29]. These processes result in a shoaling of the planetary boundary layer (PBL) over the ocean [16•, 20••, 49, 50]. In addition, the role of suppressed cloud-top entrainment due to the additional downwelling longwave flux from the enhanced CO₂ has also been suggested as important to PBL shoaling [16•, 51, 52]. These processes result in a vertical drying–moistening contrast within the lower troposphere (Fig. 1) [9•, 20••, 28, 49] accompanying the downward shift of the low-cloud layer [7••, 20••].

Table 1 summarizes the ERF and cloud radiative components that have been estimated in the previous works [4, 7••, 9•, 10•, 53]. The robust reduction in low cloud, due to the general drying of the troposphere (Fig. 1), results in a robust positive shortwave forcing associated with the cloud adjustment (about 0.6 W m⁻² per the doubling of CO₂ concentration) [7••, 9•, 10•, 54]. Longwave radiation is also an important part of the cloud adjustment, but the longwave component of cloud adjustment has been estimated to be smaller than the shortwave component (Table 1) [7••, 10•, 54]. The longwave component of the cloud radiative effect (CRE), defined as the difference of all-sky from clear-sky radiative flux at the TOA, has been estimated to be negative (about -0.8 W m⁻² per doubling of CO₂; Table 1) [4, 9•, 53]. However, such estimations demand scrutiny because the CRE can vary even when clouds do not change [55, 56]. For example, the reduction of outgoing longwave radiation due to an increase in CO₂ can be partially masked by the presence of clouds, resulting in a

reduction in CRE that is not due to cloud changes. The cloud-masking effect makes a large contribution to the longwave component of the estimated CRE (hereafter, LWCRE) [16•]. Longwave radiative forcing due to the cloud adjustment, excluding the cloud-masking effect, has been evaluated in some studies (Table 1) [7••, 10•]. Derived results have revealed that (1) both the strength and intermodel spread of longwave cloud radiative forcing are smaller than the shortwave component and the net cloud radiative forcing is dominated by the shortwave component (Table 1) and (2) the sign of longwave radiative forcing is inconsistent among the multi models [7••, 10•, 54]. In this review paper, the shortwave and longwave components of the CRE (SWCRE and LWCRE, respectively) are presented in later subsections.

Changes in the thermodynamic profiles of the troposphere are also important for the rapid adjustment of the hydrological cycle to increasing levels of CO₂. Figure 2 shows the mechanism of slowdown of the global-mean hydrological cycle as part of the rapid adjustment to an increase in CO₂. Spatial properties of the adjustment are detailed in later subsections. The changes in the vertical profiles of the tropospheric temperature and specific humidity (Fig. 1) are important for the adjustment in the hydrological cycle (Fig. 2). The strengthening of stability induces weakening of convective activity and precipitation [38, 40]. In addition, the suppressed convection leads to a moistening of the marine boundary layer and decreased evaporation and a drying of the free troposphere [20••, 42•]. The surface air over the ocean also shows rapid moistening on a daily timescale [20••, 42•], resulting in a rapid decrease in the evaporation over the ocean. These processes associated with the slowdown of global-mean hydrological cycle [9•, 16•, 20••, 21, 27, 32, 37, 42•, 57] can also be interpreted from an atmospheric energy budget perspective [5, 19•, 30, 31, 33–36, 38–40, 58, 59]. Variation in global precipitation is closely associated with net atmospheric energy balance because condensational heating is part of the atmospheric energy budget. The weakening of atmospheric radiative cooling due to increasing levels of CO₂ results in the

Table 1 Summary of ERF and cloud radiative forcing estimates due to doubling of CO₂ concentration and their spreads among multi model ensembles

Method	Number	MIP	ERF (W m ⁻²)	Net cloud forcing (W m ⁻²)	Longwave cloud forcing (W m ⁻²)	Shortwave cloud forcing (W m ⁻²)	Reference
Regression	10	CMIP3/CFMIP1	3.33±0.47	-0.36±0.47 ^a	-0.85±0.21 ^a	0.49±0.41 ^a	Gregory and Webb (2008) [4]
Regression	15	CMIP5/CFMIP2	3.45±0.56	-0.39±0.39 ^a	-0.78±0.30 ^a	0.39±0.60 ^a	Andrews et al. (2012) [53]
Fixed-SST	7	CMIP5/CFMIP2	3.51±0.47	-	-	-	Andrews et al. (2012) [53]
Fixed-SST	13	CMIP5/CFMIP2	3.77±0.45	-0.15±0.26 ^a	-0.76±0.11 ^a	0.62±0.24 ^a	Kamae and Watanabe (2012) [9•]
Fixed-SST	8	CMIP5/CFMIP2	3.75±0.42	0.41±0.28	-0.13±0.24	0.54±0.45	Vial et al. (2013) [10•]
Fixed-SST	5	CMIP5/CFMIP2	-	0.53±0.34	-0.03±0.13	0.56±0.29	Zelinka et al. (2013) [7••]

Numbers in column “number” represent model numbers used in the estimates. The MIP column denotes the model intercomparison project in which the models participated

^a Cloud radiative forcing estimated by CRE method. Uncertainties are ±1 standard deviations of the multi-model ensembles

Slowdown of hydrological cycle

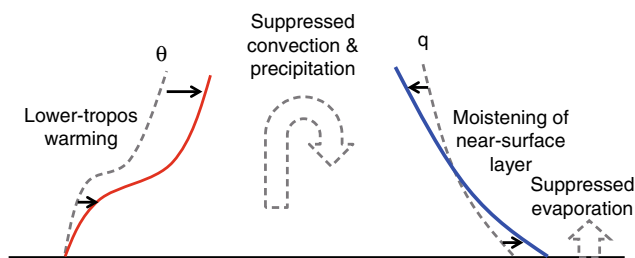


Fig. 2 Schematics of rapid adjustment of the global hydrological cycle to increasing CO_2 over the ocean. θ and q are potential temperature and specific humidity, respectively. Pairs of gray dashed and colored solid lines represent vertical profiles under the control and CO_2 -increased conditions. Dashed arrows represent reductions of convection and evaporation

decrease of the global precipitation. In addition, land–sea contrast is also an important factor for geographical pattern of the response of the hydrological cycle to increasing CO_2 (detailed in a later subsection).

Timescales of Global and Regional Adjustments

In contrast to the slow timescale (of the order of a year to a decade) of cloud response to external forcing (i.e., SAT-mediated cloud change), the timescale of cloud adjustment to increasing levels of CO_2 had been thought to be shorter than a year [60]. Rapid processes related to direct tropospheric responses to increasing levels of CO_2 can be examined using large-member ensemble AGCM simulations (i.e., the short ensemble simulation introduced above) [41]. Figure 3 shows time evolutions of global-mean adjustments (SWCRE, LWCRE, precipitation, and evaporation) examined by 64-member ensemble 10-day integrations and the equilibrium response (30-year mean) [20••] derived from an AGCM [61]. Global-mean adjustments in SWCRE and LWCRE approach their equilibrium states within 2 days (Fig. 3b) [20••]. The global hydrological cycle (precipitation and evaporation) also responds on a daily timescale (Fig. 3c) [19•, 20••, 42•]. This is because atmospheric radiative heating due to instantaneous CO_2 forcing [28, 48] can rapidly warm the troposphere, resulting in tropospheric adjustment on a short timescale [20••], including a “vertical stratification process” within the troposphere (Figs. 1 and 2) [6].

However, spatial patterns of responses simulated in the long-term AGCM integration cannot be fully explained by the daily-scale responses. Figure 4 shows spatial distributions of the daily-scale and long-term responses to abruptly increased CO_2 concentration. Although the global-mean adjustments of CRE, precipitation and evaporation approach their long-term means within days to a week (Fig. 3b, c), and geographical patterns of daily-scale adjustments are somewhat different from the equilibrium changes (Fig. 4). For example,

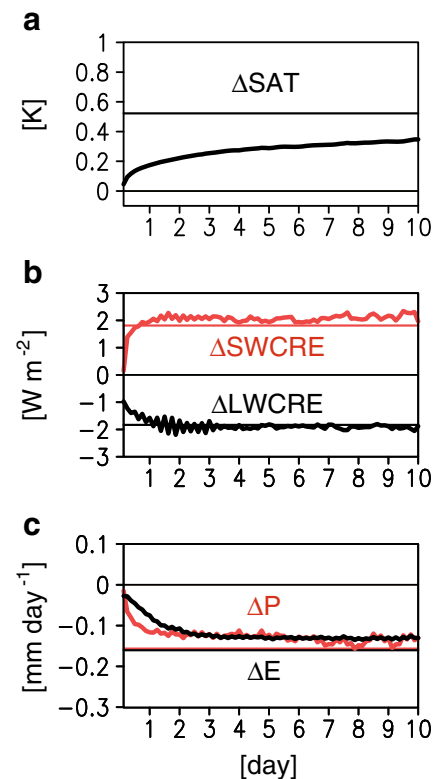
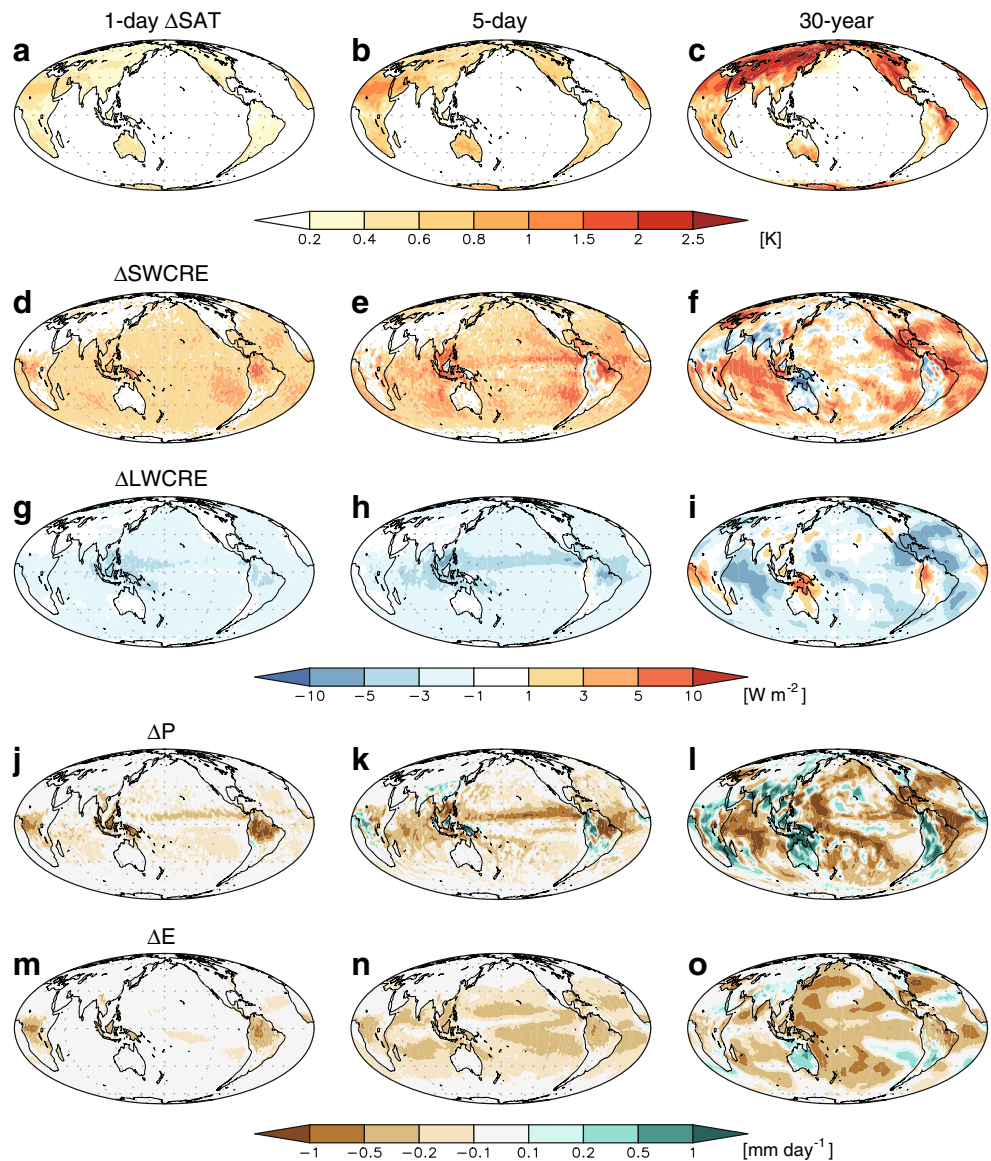


Fig. 3 Time-series of global-mean adjustments to abruptly quadrupled CO_2 concentration simulated in MIROC5 AGCM. Thick curves represent 64-member means of the short ensemble simulation. Thin lines are 30-year means. **a** SAT, **b** SWCRE and LWCRE, and **c** precipitation and evaporation. Modified from: Kamae Y, Watanabe M (2013) Tropospheric adjustment to increasing CO_2 : its timescale and the role of land–sea contrast. *Clim Dyn* 41:3007–3024

SWCRE response within 5 days shows a general increase over the ocean (Fig. 4e), but the equilibrium response (Fig. 4f) shows a spatially asymmetric pattern (i.e., large increases over the Indian Ocean, Atlantic Ocean, and the eastern subtropical Pacific and small change over the western and central Pacific). As for the daily-scale response of precipitation, reduction over the ocean is larger over the tropical convective regions than the subtropics (Fig. 4k) [19•], but this feature is not clear in the long-term response (Fig. 4l). Interestingly, the spatial pattern of the long-term precipitation response is similar to that of SWCRE (Fig. 4f, l). Over the land, adjustments of CRE and hydrological cycle tend to show opposite signs to those over the ocean (i.e., negative and positive responses of SWCRE and precipitation over the land) [9•, 20••].

One of the reasons for the spatial non-uniformity in the adjustment is change in large-scale atmospheric circulation [16•, 20••, 21]. In particular, gradual change in land–sea thermal contrast (Fig. 4a–c) [20••, 41] is one of the reasons for the differences between the spatial patterns of adjustments found on a daily timescale (Fig. 4e, h, k, and n) and the equilibrium response (Fig. 4f, i, l, and o). The role of the gradual response

Fig. 4 Time evolutions of geographical patterns of the rapid adjustments simulated in MIROC5 AGCM. **a, d, g, j, m** 1-day and **b, e, h, k, n** 5-day means of rapid adjustments. **c, f, i, l, o** 30-year means. **a–c** SAT, **d–f** SWCRE, **g–i** LWCRE, **j–l** precipitation, and **m–o** evaporation. Modified from: Kamae Y, Watanabe M (2013) Tropospheric adjustment to increasing CO₂: its timescale and the role of land–sea contrast. *Clim Dyn* 41:3007–3024



to CO₂ forcing over land (Fig. 4a–c) on cloud change is discussed in the following subsection.

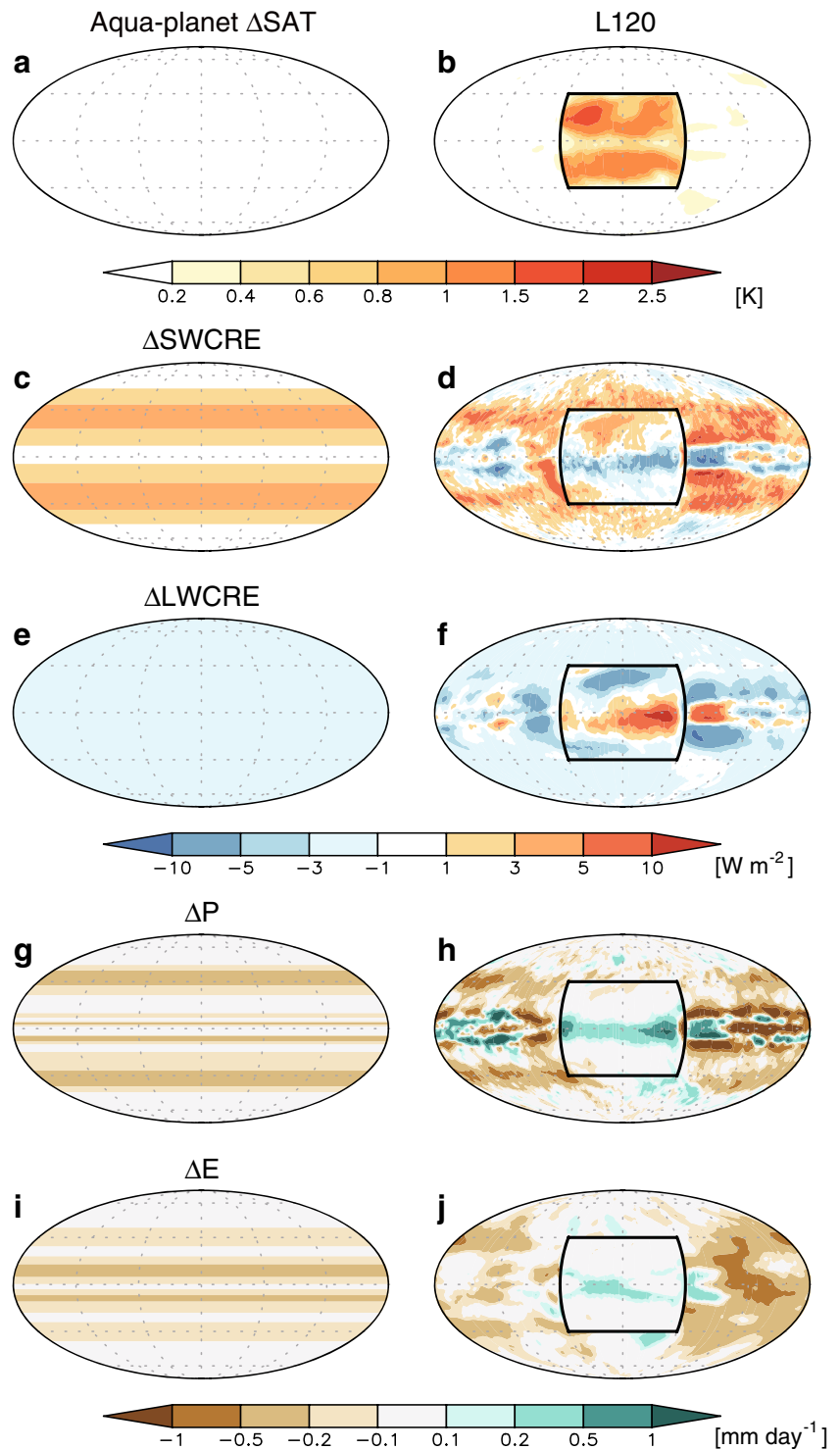
Role of Land Surface Response

In the fixed-SST method, the land surface warms in response to the increased CO₂ concentration, resulting in a land–sea surface warming contrast (Fig. 4c) [4, 16, 20, 41]. It is not strictly accurate to include additional responses associated with land surface warming as part of the adjustment processes. Land surface temperature should be fixed in order to isolate the radiative perturbation due to increasing CO₂ [44]; however, this method has not been applied to other model simulations because of the difficulty of its implementation [8]. This land–sea thermal contrast can evoke anomalous atmospheric circulation (upward/downward motions over the land/ocean),

cloud [16, 20, 62], and precipitation patterns [21]. Increasing cloud amount via enhanced deep convection over the land [16] results in a negative SWCRE response over the land (Fig. 4f) despite the positive global-mean response of SWCRE (Fig. 3b, Table 1) [20]. However, tropospheric cloud adjustment can also be found in aqua-planet models [20, 57, 63] (detailed below), suggesting that the effect of changing land–sea thermal contrast is not necessary for cloud adjustment.

Here, the role of land in the cloud response can be examined using aqua-planet both with and without an ideal rectangular continent over the tropics [20]. Figure 5 shows the climate responses to increasing CO₂ simulated in an aqua-planet both with and without a continent that has longitudinal width of 120° over the tropics (30° S–30° N). Table 2 summarizes adjustments averaged over the tropics, tropical land, and tropical ocean areas. SWCRE and LWCRE adjustments

Fig. 5 Adjustments in aqua-planet (**b, d, f, h, j**) with and (**a, c, e, g, i**) without rectangular continent with 120° longitudinal width (L120) in the tropics (30° S–30° N) simulated in MIROC5 aqua-planet model. *Black lines* represent land shapes. **a–b** SAT, **c–d** SWCRE, **e–f** LWCRE, **g–h** precipitation, and **i–j** evaporation. Modified from: Kamae Y, Watanabe M (2013) Tropospheric adjustment to increasing CO₂: its timescale and the role of land-sea contrast. *Clim Dyn* 41:3007–3024



over the equatorial land region show opposite signs to those found in the aqua-planet (Fig. 5c–f), resulting in smaller adjustments in L120 than the aqua-planet (Table 2). In the AGCM, the ocean-mean cloud adjustments are also larger than the tropical-mean adjustments (Fig. 5, Table 2), suggesting that the land surface responses dampen the tropical-mean CRE response [20••]. Other model simulations also revealed

that CRE adjustments in aqua-planet are generally larger than AGCM with realistic continents [57, 63]. The enhanced deep convection and associated increase in high cloud (and precipitation and evaporation; Fig. 5h, j) over the land, in response to land surface warming (Figs. 4c and 5b) [16•, 20••], induces opposite signs of SWCRE and LWCRE responses over the land areas to those found in the aqua-planet (Fig. 5c–f).

Table 2 Tropical-mean (30° S–30° N) adjustments in MIROC5 aqua-planet (Fig. 5c, e), AGCM (Fig. 4f, i), and aqua-planet with a rectangular continent with 120° longitudinal width (L120) in the tropics (30° S–30° N; Fig. 5d, f)

		Aqua-planet	AGCM	L120
Δ SWCRE (W m ⁻²)	Tropics	2.74±0.18	2.28±0.52	1.29±0.21
	Ocean	2.74±0.18	2.86±0.51	2.04±0.14
	Land	–	0.48±0.51	–0.52±0.41
Δ LWCRE (W m ⁻²)	Tropics	–1.95±0.18	–2.06±0.46	–1.67±0.18
	Ocean	–1.95±0.18	–2.46±0.45	–2.18±0.22
	Land	–	–0.77±0.45	–0.43±0.35

Ocean and *land* represent averages over the tropical-ocean (30° S–30° N) and tropical-land areas, respectively. Uncertainties are ±1 standard deviations in interannual variabilities

These characters of the adjustment over the land associated with the land warming can also be found in the AGCM simulation (Fig. 4). The global-mean CRE simulated in the AGCMs can be interpreted as the sum of the adjustments in the aqua-planet and the effect of the land surface warming [20••]. However, results of sensitivity simulations with differing sizes of continents suggest that the damping effect due to land warming is not a critical process for tropospheric cloud adjustment [20••].

It should be noted that the land effect on the climate response is also associated with CO₂ physiological processes [5, 41, 60, 64–66]. In response to increasing CO₂ concentration in the atmosphere, CO₂ used in photosynthesis gains easier entry into the leaf via the stomata, resulting in the closures of stomata and the reduction of evapotranspiration from land plants, particularly in the low-latitude regions. The reduction of evapotranspiration can be found just after the CO₂ increase (Fig. 4m) [20••, 41, 42•]. This dampening of water vapor release from the land surface suppresses precipitation over tropical land areas (Fig. 4j). These CO₂-induced physiological processes have been examined and compared with physical processes via sensitivity simulations with fixed and variable stomatal resistances [41, 42•, 49, 60]. The reduction of land surface evapotranspiration due to physiological processes results in (1) additional surface and tropospheric warming over the land and associated changes in atmospheric circulation and (2) reduction of low cloud over land and increasing positive SWCRE [41, 49]. The influence of CO₂ physiological forcing is an important factor in the changes of the hydrological cycle and cloud amount particularly over tropical land areas.

The responses to increasing CO₂ over the land detailed above (e.g., SAT; Fig. 4a, b) are also important for the transient climate changes. In response to the transient radiative forcing, the land surface warming simulated in AOGCMs is generally larger than the sea surface warming [67, 68] because of differences in thermal inertia, boundary-layer lapse rate,

and surface energy budget between the land and ocean [67, 69, 70]. Here, the direct response to the CO₂ forcing over the land (Fig. 4a, b) is essential for the land surface warming particularly over the Northern Hemisphere (NH) extratropics [22, 71, 72]. As a result, projected future changes in the land–sea thermal contrast and associated atmospheric circulation over the NH extratropics [73–75] are clearly affected by the direct land response to the CO₂ forcing [71]. In addition, the direct response to the CO₂ forcing is also important for the past climate changes [14, 22, 72]. Contribution of the direct land response to anthropogenically induced external forcing (CO₂, aerosols, and land-use change) on the recent increase in SAT and frequency of hot summers over the NH land areas was found to be robust [22, 72]. These findings [14, 22, 71–75] explained new aspects of the direct climate response to the external forcing including the rapid tropospheric adjustment.

Possible Factors for Intermodel Spread of Adjustment

Combinations of the fixed-SST method, regression method, and aqua-planet simulations (see previous subsection) have enabled the quantitative assessment of the cloud adjustment and the evaluation of possible factors related to intermodel spread. Assessments of the radiative effect of the cloud adjustment have revealed that the influence of intermodel spread of the cloud adjustment on the uncertainty in the ECS is smaller than that of SAT-mediated cloud change [9•, 10•, 29, 53]. In response to increasing levels of CO₂, the rapid adjustments of lower tropospheric stability (LTS) and estimated inversion strength (EIS) were found to be generally positive [29], except for one model in which biases in radiative heating rate resulted in unusual adjustments of LTS and EIS [48]. As LTS and EIS are measures that are highly correlated with the amount of stratus in the present climate, these results suggest that the vertical profile of instantaneous radiative forcing could be a factor in the uncertainty of the cloud adjustment.

The robustness of the cloud adjustment between models participating in the Coupled Model Intercomparison Project phase 5 (CMIP5) [46] has been examined in detail [9•]. Figure 6 shows the changes in SWCRE and lower-tropospheric RH associated with the cloud adjustment. The reduction of cloud amount (Fig. 1), positive SWCRE (Table 1; Figs. 4d–f and 6), tropospheric warming and drying (Figs. 1 and 6), and moistening of the near-surface layer over the ocean (Fig. 1) are robust features among the models [9•]. In comparison with the SAT-mediated cloud change, the signs of the SWCRE adjustment are more robust [7••], but the strength varies substantially between the models (Fig. 6) [9•]. This intermodel spread of the SWCRE is the largest contributor to the total intermodel spread of the net ERF [9•] and

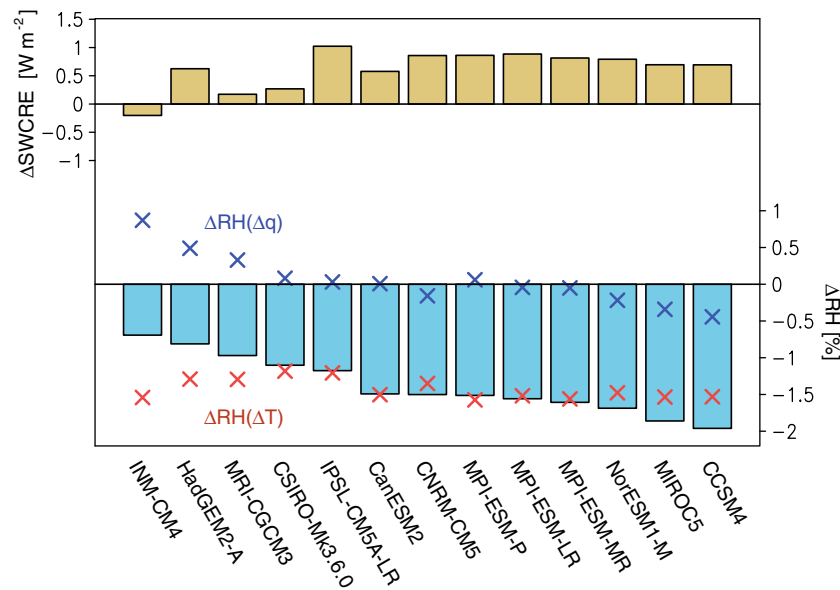


Fig. 6 SWCRE and change in lower-tropospheric RH (700–925 hPa) associated with tropospheric adjustment to increasing CO_2 simulated in 13 CMIP5 models. SWCRE is scaled to be $2 \times \text{CO}_2$ equivalent (similar to Table 1). Changes in RH are averages in subsidence regime over the tropical ocean (30°S – 30°N). Red and blue crosses represent

components of RH change driven by change in temperature and specific humidity, respectively. Modified from: Kamae Y, Watanabe M (2012) On the robustness of tropospheric adjustment in CMIP5 models. *Geophys Res Lett* 39:L23808. doi:10.1029/2012GL054275

corresponds mainly to the spread of change in the lower tropospheric RH over the ocean (Fig. 6). This RH spread is induced primarily by the spread of change in specific humidity over the region of tropical subsidence (Fig. 6). However, the physical processes governing this intermodel spread of lower tropospheric specific humidity over the region of tropical subsidence are not clear [9•]. Some models have considerable biases in their vertical profiles of cloud ice and liquid water compared with satellite observations [76]. Such large biases could contribute to discrepancies in the rapid cloud adjustment from other models [9•]. The possible influences of other factors, e.g., evaporation from the sea surface, turbulent mixing within the boundary layer over the ocean, shallow convection, and large-scale atmospheric circulations, should be examined further in future studies. For example, efficiency of convective dehydration of the PBL via a lower-tropospheric mixing can be a source of uncertainty in the boundary-layer cloud response to the external forcing simulated in climate models [77].

The relationship between the intermodel spread of the cloud radiative component of the ERF and that of cloud feedback parameter has received considerable attention [29]. The relationship between the ERF and total feedback parameter of the CMIP5 GCMs shows a significant anticorrelation [63]. Namely, models with larger ERF tend to have larger negative feedback parameter and vice versa. Such a relationship has also been confirmed in physics parameter perturbation ensembles [29, 78]. The cancellation results in a reduction of the intermodel spread of the ECS from that suggested by the

intermodel spreads of the feedback parameter or ERF alone. In addition, clear anticorrelation between the CRE components of the ERF and feedback can also be found in aquaplanet models [63]. Further studies are needed to explore both the possible mechanisms for such anticorrelation and the reasons for the uncertainties in the cloud adjustment and resultant ECS.

Conclusions

Our understanding of the physical mechanisms of rapid cloud and climate adjustments has advanced considerably because of extensive research. One reason for the progress is the development of a systematic experimental framework (including fixed-SST and regression methods and aqua-planet configuration) [7••, 9•, 19•, 20••, 53, 57, 63] with which to examine the rapid cloud adjustment under the Cloud Feedback Model Intercomparison Project phase 2 (CFMIP2)/CMIP5 protocol [46]. The short ensemble simulations [19•, 20••] also contribute to improve the process-based interpretation of the rapid adjustment. The derived results have revealed the robustness of the tropospheric cloud adjustment [7••, 9•, 57]. However, the remaining issues on the sources of uncertainty in the cloud adjustment (e.g., instantaneous radiative perturbation, PBL dehydration, and associated changes in cloud radiative properties) [7••, 9•, 29, 48, 63, 77] are still important for the assessment of uncertainty in the ECS [29, 63]. Unfortunately, it is not easy to assess reliability of the adjustment processes derived from the modeling studies by comparing with

observational records. However, detailed comparisons with responses simulated in less parameterized models [16•, 51, 52] may contribute to assess confidence of the current understanding of the mechanism of the cloud adjustment.

In this review, processes associated with adjustment to solar irradiance [21, 36, 37, 42•] and spatially inhomogeneous forcing factors such as aerosols and ozone [36, 79–82] have not been included. Both the direct responses and SAT-mediated changes to the external forcing agents (including CO₂ and other forcing factors) are important for the changes in large-scale atmospheric circulations (e.g., tropical atmospheric circulation, mid-latitude westerlies, and stratospheric circulation) [12–15, 16•, 17, 18, 19•, 20••, 21–23, 80] and hydrological cycle [36, 80, 81]. Comprehensive approaches for better understanding of the direct and SAT-mediated climate responses are important future works. Such framework may provide significant implications for broad scientific areas not limited to the uncertainties in the ECS and transient climate response [82] but detection and attribution, atmospheric chemistry, paleoclimate, and geoengineering.

Acknowledgments This work was supported by the Program for Risk Information on Climate Change (SOUSEI program) and Grant-in-Aid 26281013 from the Ministry of Education, Culture, Sports, Science, and Technology (MEXT), Japan, and the Environment Research and Technology Development Fund (S-10) of the Ministry of the Environment of Japan.

Conflict of Interest On behalf of all authors, the corresponding author states that there is no conflict of interest.

Open Access This article is distributed under the terms of the Creative Commons Attribution License which permits any use, distribution, and reproduction in any medium, provided the original author(s) and the source are credited.

References

Papers of particular interest, published recently, have been highlighted as:

- Of importance
- Of major importance

1. Knutti R, Hegerl GC. The equilibrium sensitivity of the Earth's temperature to radiation changes. *Nat Geosci.* 2008;1:735–43.
2. Maslin M, Austin P. Uncertainty: climate models at their limit? *Nature.* 2012;486:183–4.
3. Boucher O, Randall D, Artaxo P, et al. Clouds and aerosols. In: Stocker TF, editor. *Climate change 2013: the physical science basis. Contribution of working group I to the Fifth Assessment Report of the Intergovernmental Panel on Climate Change.* Cambridge: Cambridge University Press; 2014. p. 571–658.
4. Gregory JM, Webb MJ. Tropospheric adjustment induces a cloud component in CO₂ forcing. *J Clim.* 2008;21:58–71.

5. Andrews T, Gregory JM, Forster PM, Webb MJ. Cloud adjustment and its role in CO₂ radiative forcing and climate sensitivity: a review. *Surv Geophys.* 2012;33:619–35.
6. Sherwood SC, Bony S, Boucher O, Bretherton C, Forster PM, Gregory JM, et al. Adjustments in the forcing–feedback framework for understanding climate change. *Bull Am Meteorol Soc.* 2014. doi:10.1175/BAMS-D-13-00167.1.
7. Zelinka MD, Klein SA, Taylor KE, Andrews T, Webb MJ, Gregory JM, et al. Contributions of different cloud types to feedbacks and rapid adjustments in CMIP5. *J Clim.* 2013;26:5007–27. *Using a cloud radiative kernel, this study revealed roles of different cloud heights and cloud optical depths in the rapid adjustment.*
8. Hansen J, Sato M, Ruedy R, et al. Efficacy of climate forcings. *J Geophys Res.* 2005;110, D18104. doi:10.1029/2005JD005776.
9. Kamae Y, Watanabe M. On the robustness of tropospheric adjustment in CMIP5 models. *Geophys Res Lett.* 2012;39, L23808. doi:10.1029/2012GL054275. *This study explored robustness of the tropospheric adjustment and identified one of the sources of uncertainty.*
10. Vial J, Dufresne J-L, Bony S. On the interpretation of inter-model spread in CMIP5 climate sensitivity estimates. *Clim Dyn.* 2013;41:3339–62. *Using NCAR model's radiative kernel, this study explored relative contributions of the adjustment on the temperature change and the ECS uncertainty.*
11. Folland CK, Sexton DMH, Karoly DJ, Johnson CE, Rowell DP, Parker DE. Influences of anthropogenic and oceanic forcing on recent climate change. *Geophys Res Lett.* 1998;25:353–6.
12. Bracco A, Kucharski F, Kallummal R, Molteni F. Internal variability, external forcing and climate trends in multi-decadal AGCM ensembles. *Clim Dyn.* 2004;23:659–78.
13. Kodama C, Iwasaki T, Shibata K, Yukimoto S. Changes in the stratospheric mean meridional circulation due to increased CO₂: radiation- and sea surface temperature-induced effects. *J Geophys Res.* 2007;112, D16103. doi:10.1029/2006JD008219.
14. Deser C, Phillips AS. Atmospheric circulation trends, 1950–2000: the relative roles of sea surface temperature forcing and direct atmospheric radiative forcing. *J Clim.* 2009;22:396–413.
15. Kawatani Y, Hamilton K, Noda A. The effects of changes in sea surface temperature and CO₂ concentration on the quasi-biennial oscillation. *J Atmos Sci.* 2012;69:1734–49.
16. Wyant MC, Bretherton CS, Blossey PN, Khairoutdinov M. Fast cloud adjustment to increasing CO₂ in a superparameterized climate model. *J Adv Model Earth Syst.* 2012;4:M05001. doi:10.1029/2011MS000092 *This study examined cloud adjustment to CO₂ increase using super parameterized climate model and explored the processes related to PBL shoaling.*
17. Wu Y, Seager R, Ting M, Naik N, Shaw TA. Atmospheric circulation response to an instantaneous doubling of carbon dioxide. Part I: model experiments and transient thermal response in the troposphere. *J Clim.* 2012;25:2862–79.
18. Wu Y, Seager R, Shaw TA, Ting M, Naik N. Atmospheric circulation response to an instantaneous doubling of carbon dioxide. Part II: atmospheric transient adjustment and its dynamics. *J Clim.* 2013;26:918–35.
19. Bony S, Bellon G, Klocke D, Sherwood S, Fermepein S, Denvil S. Robust direct effect of carbon dioxide on tropical circulation and regional precipitation. *Nat Geosci.* 2013;6:447–451. doi:10.1038/ngeo1799 *This study revealed robustness of direct responses to CO₂ increase in tropical atmospheric circulation and precipitation on different timescales.*
20. Kamae Y, Watanabe M. Tropospheric adjustment to increasing CO₂: its timescale and the role of land–sea contrast. *Clim Dyn.* 2013;41:3007–24. *Using short ensemble and idealized simulations, this study clearly explored the rapid processes of adjustment and role of the increasing land–sea thermal contrast.*

21. Chadwick R, Good P, Andrews T, Martin G. Surface warming patterns drive tropical rainfall pattern responses to CO₂ forcing on all timescales. *Geophys Res Lett*. 2014;41:610–5.
22. Kamae Y, Shiogama H, Watanabe M, Kimoto M. Attributing the increase in Northern Hemisphere hot summers since the late 20th century. *Geophys Res Lett*. 2014;41:5192–9.
23. Grise KM, Polvani LM. The response of mid-latitude jets to increased CO₂: distinguishing the roles of sea surface temperature and direct radiative forcing. *Geophys Res Lett*. 2014;41:6863–71.
24. Yoshimura J, Sugi M. Tropical cyclone climatology in a high-resolution AGCM—impacts of SST warming and CO₂ increase. *SOLA*. 2005;1:133–6.
25. Held IM, Zhao M. The response of tropical cyclone statistics to an increase in CO₂ with fixed sea surface temperatures. *J Clim*. 2011;24:5353–64.
26. Scoccimarro E, Gualdi S, Villarini G, Vecchi GA, Zhao M, Walsh K, et al. Intense precipitation events associated with landfalling tropical cyclones in response to a warmer climate and increased CO₂. *J Clim*. 2014;27:4642–54.
27. Andrews T, Forster PM. CO₂ forcing induces semi-direct effects with consequences for climate feedback interpretations. *Geophys Res Lett*. 2008;35, L04802. doi:10.1029/2007GL032273.
28. Colman RA, McAvaney BJ. On tropospheric adjustment to forcing and climate feedbacks. *Clim Dyn*. 2011;36:1649–58.
29. Webb MJ, Lambert FH, Gregory JM. Origins of differences in climate sensitivity, forcing and feedback in climate models. *Clim Dyn*. 2013;40:677–707.
30. Mitchell JFB, Wilson CA, Cunningham WM. On CO₂ climate sensitivity and model dependence of results. *Q J R Meteorol Soc*. 1987;113:293–322.
31. Allen MR, Ingram WJ. Constraints on future changes in climate and the hydrologic cycle. *Nature*. 2002;419:224–32.
32. Yang F, Kumar A, Schlesinger ME, Wang W. Intensity of hydrological cycles in warmer climates. *J Clim*. 2003;16:2419–23.
33. Sugi M, Yoshimura J. A mechanism of tropical precipitation change due to CO₂ increase. *J Clim*. 2004;17:238–43.
34. Lambert FH, Webb MJ. Dependency of global mean precipitation on surface temperature. *Geophys Res Lett*. 2008;35, L16706. doi:10.1029/2008GL034838.
35. Andrews T, Forster PM, Gregory JM. A surface energy perspective on climate change. *J Clim*. 2009;22:2557–70.
36. Andrews T, Forster PM, Boucher O, Bellouin N, Jones A. Precipitation, radiative forcing and global temperature change. *Geophys Res Lett*. 2010;37, L14701. doi:10.1029/2010GL043991.
37. Bala G, Caldeira K, Nemani R. Fast versus slow response in climate change: implications for the global hydrological cycle. *Clim Dyn*. 2010;35:423–34.
38. O’Gorman PA, Allan RP, Byrne MP, Previdi M. Energetic constraints on precipitation under climate change. *Surv Geophys*. 2012;33:585–608.
39. Kvalevåg MM, Samset BH, Myhre G. Hydrological sensitivity to greenhouse gases and aerosols in a global climate model. *Geophys Res Lett*. 2013;40:1432–8.
40. Allan RP, Liu C, Zahn M, Lavers DA, Koukouvasias E, Bodas-Salcedo A. Physically consistent responses of the global atmospheric hydrological cycle in models and observations. *Surv Geophys*. 2014;35:533–52.
41. Dong B, Gregory JM, Sutton RT. Understanding land–sea warming contrast in response to increasing greenhouse gases. Part I: transient adjustment. *J Clim*. 2009;22:3079–97.
42. Cao L, Bala G, Caldeira K. Climate response to changes in atmospheric carbon dioxide and solar irradiance on the time scale of days to weeks. *Environ Res Lett*. 2012;7, 034015. *Using a large-member ensemble simulation conducted in an AOGCM, this study examined processes of the rapid adjustment in hydrological cycle.*
43. Hansen J, Sato M, Nazarenko L, et al. Climate forcings in Goddard Institute for Space Studies SI2000 simulations. *J Geophys Res*. 2002;107:4347. doi:10.1029/2001JD001143.
44. Shine KP, Cook J, Highwood EJ, Joshi MM. An alternative to radiative forcing for estimating the relative importance of climate change mechanisms. *Geophys Res Lett*. 2003;30:2047. doi:10.1029/2003GL018141.
45. Gregory JM, Ingram WJ, Palmer MA, et al. A new method for diagnosing radiative forcing and climate sensitivity. *Geophys Res Lett*. 2004;31, L03205. doi:10.1029/2003gl018747.
46. Taylor KE, Stouffer RJ, Meehl GA. An overview of CMIP5 and the experiment design. *Bull Am Meteorol Soc*. 2012;93:485–98.
47. Collins WD, Ramaswamy V, Schwarzkopf MD, et al. Radiative forcing by well-mixed greenhouse gases: estimates from climate models in the Intergovernmental Panel on Climate Change (IPCC) fourth assessment report (AR4). *J Geophys Res*. 2006;111, D14317. doi:10.1029/2005JD006713.
48. Ogura T, Webb MJ, Watanabe M, Lambert FH, Tsushima Y, Sekiguchi M. Importance of instantaneous radiative forcing for rapid tropospheric adjustment. *Clim Dyn*. 2014;43:1409–21.
49. Andrews T, Ringer MA. Cloud feedbacks, rapid adjustments, and the forcing–response relationship in a transient CO₂ reversibility scenario. *J Clim*. 2014;27:1799–818.
50. Watanabe M, Shiogama H, Yoshimori M, Ogura T, Yokohata T, Okamoto H, et al. Fast and slow timescales in the tropical low-cloud response to increasing CO₂ in two climate models. *Clim Dyn*. 2012;39:1627–41.
51. Bretherton CS, Blossey PN, Jones CR. Mechanisms of marine low cloud sensitivity to idealized climate perturbations: a single-LES exploration extending the CGILS cases. *J Adv Model Earth Syst*. 2013;5:316–37.
52. Bretherton CS, Blossey PN. Low cloud reduction in a greenhouse-warmed climate: results from Lagrangian LES of a subtropical marine cloudiness transition. *J Adv Model Earth Syst*. 2014;6:91–114.
53. Andrews T, Gregory JM, Webb MJ, Taylor KE. Forcing, feedbacks and climate sensitivity in CMIP5 coupled atmosphere–ocean climate models. *Geophys Res Lett*. 2012;39, L09712. doi:10.1029/2012GL051607.
54. Tomassini L, Geoffroy O, Dufresne J-L, et al. The respective roles of surface temperature driven feedbacks and tropospheric adjustment to CO₂ in CMIP5 transient climate simulations. *Clim Dyn*. 2013;41:3103–26.
55. Soden BJ, Broccoli AJ, Hemler RS. On the use of cloud forcing to estimate cloud feedback. *J Clim*. 2004;17:3661–5.
56. Soden BJ, Held IM, Colman R, Shell KM, Kiehl JT, Shields CA. Quantifying climate feedbacks using radiative kernels. *J Clim*. 2008;21:3504–20.
57. Medeiros B, Stevens B, Bony S. Using aquaplanets to understand the robust responses of comprehensive climate models to forcing. *Clim Dyn*. 2014. doi:10.1007/s00382-014-2138-0.
58. Takahashi K. The global hydrological cycle and atmospheric short-wave absorption in climate models under CO₂ forcing. *J Clim*. 2009;22:5667–75.
59. Pendergrass AG, Hartmann DL. The atmospheric energy constraint on global-mean precipitation change. *J Clim*. 2014;27:757–68.
60. Doutriaux-Boucher M, Webb MJ, Gregory JM, Boucher O. Carbon dioxide induced stomatal closure increases radiative forcing via a rapid reduction in low cloud. *Geophys Res Lett*. 2009;36, L02703. doi:10.1029/2008GL036273.
61. Watanabe M, Suzuki T, O’ishi R, et al. Improved climate simulation by MIROC5: mean states, variability, and climate sensitivity. *J Clim*. 2010;23:6312–135.
62. Lambert FH, Webb MJ, Joshi MM. The relationship between land–ocean surface temperature contrast and radiative forcing. *J Clim*. 2011;24:3239–56.

63. Ringer MA, Andrews T, Webb MJ. Global-mean radiative feedbacks and forcing in atmosphere-only and coupled atmosphere-ocean climate change experiments. *Geophys Res Lett*. 2014;41:4035–42.
64. Sellers PJ, Bounoua L, Collatz GJ, Randall DA, Dazlich DA, Los SO, et al. Comparison of radiative and physiological effect of doubled atmospheric CO₂ on climate. *Science*. 1996;271:1402–6.
65. Boucher O, Jones A, Betts RA. Climate response to the physiological impact of carbon dioxide on plants in the Met Office Unified Model HadCM3. *Clim Dyn*. 2009;32:237–49.
66. Andrews T, Doutriaux-Boucher M, Boucher O, Forster PM. A regional and global analysis of carbon dioxide physiological forcing and its impact on climate. *Clim Dyn*. 2011;36:783–92.
67. Manabe S, Stouffer RJ, Spelman MJ, Bryan K. Transient responses of a coupled ocean–atmosphere model to gradual changes of atmospheric CO₂. Part I: annual mean response. *J Clim*. 1991;4:785–818.
68. Sutton RT, Dong B, Gregory JM. Land/sea warming ratio in response to climate change: IPCC AR4 model results and comparison with observations. *Geophys Res Lett*. 2007;34, L02701. doi:10.1029/2006GL028164.
69. Joshi MM, Gregory JM, Webb MJ, Sexton DMH, Johns TC. Mechanisms for the land/sea warming contrast exhibited by simulations of climate change. *Clim Dyn*. 2008;30:455–65.
70. Joshi MM, Lambert FH, Webb MJ. An explanation for the difference between twentieth and twenty-first century land–sea warming ratio in climate models. *Clim Dyn*. 2013;41:1853–69.
71. Kamae Y, Watanabe M, Kimoto M, Shiogama H. Summertime land–sea thermal contrast and atmospheric circulation over East Asia in a warming climate—part II: importance of CO₂-induced continental warming. *Clim Dyn*. 2014;43:2569–83.
72. Andrews T. Using an AGCM to diagnose historical effective radiative forcing and mechanisms of recent decadal climate change. *J Clim*. 2014;27:1193–209.
73. Kimoto M. Simulated change of the East Asian circulation under the global warming scenario. *Geophys Res Lett*. 2005;32, L16701. doi:10.1029/2005GL023383.
74. Arai M, Kimoto M. Simulated interannual variation in summertime atmospheric circulation associated with the East Asian monsoon. *Clim Dyn*. 2008;31:435–47.
75. Kamae Y, Watanabe M, Kimoto M, Shiogama H. Summertime land–sea thermal contrast and atmospheric circulation over East Asia in a warming climate—part I: past changes and future projections. *Clim Dyn*. 2014;43:2553–68.
76. Jiang JH, Su H, Zhai C, et al. Evaluation of cloud and water vapor simulations in CMIP5 climate models using NASA “A-Train” satellite observations. *J Geophys Res*. 2012;117, D14105. doi:10.1029/2011JD017237.
77. Sherwood SC, Bony S, Dufresne JL. Spread in model climate sensitivity traced to atmospheric convective mixing. *Nature*. 2014;505:37–42.
78. Shiogama H, Watanabe M, Yoshimori M, et al. Perturbed physics ensemble using the MIROC5 coupled atmosphere-ocean GCM without flux corrections: experimental design and results. *Clim Dyn*. 2012;39:3041–56.
79. Shindell D, Faluvegi G. Climate response to regional radiative forcing during the twentieth century. *Nat Geosci*. 2009;2:294–300.
80. Yoshimori M, Broccoli AJ. Equilibrium response of an atmosphere-mixed layer ocean model to different radiative forcing agents: global and zonal mean response. *J Clim*. 2008;21:4399–423.
81. Shiogama H, Emori S, Takahashi K, Nagashima T, Ogura T, Nozawa T, et al. Emission scenario dependency of precipitation on global warming in the MIROC3.2 model. *J Clim*. 2010;23:2404–17.
82. Shindell D. Inhomogeneous forcing and transient climate sensitivity. *Nat Clim Chang*. 2014;4:274–7.